

## COVID-19: docking-based virtual screening and molecular dynamics study to identify potential SARS-CoV-2 spike protein inhibitors from plant-based phenolic compounds

Shirin Moradkhani<sup>1</sup>, Abbas Farmani<sup>2</sup>, Massoud Saidijam<sup>3</sup>, Amir Taherkhani<sup>4\*</sup>

<sup>1</sup>Department of Pharmacognosy, School of Pharmacy, Medicinal Plants and Natural Product Research Center, Hamadan University of Medical Sciences, Hamadan, Iran; <sup>2</sup>Dental Research Center, Hamadan University of Medical Sciences, Hamadan, Iran; <sup>3</sup>Department of Molecular Medicine and Genetics, Research Center for Molecular Medicine, Hamadan University of Medical Sciences, Hamadan, Iran; <sup>4</sup>Research Center for Molecular Medicine, Hamadan University of Medical Sciences, Hamadan, Iran

Received January 26, 2021; revised April 29, 2021; accepted July 20, 2021

**Summary.** – A novel coronavirus, known as severe acute respiratory syndrome coronavirus 2 (SARS-CoV-2), enters into the host cells through an interaction between its surface spike protein (S-protein) and the angiotensin-converting enzyme 2 receptors, leading to coronavirus disease 2019 (COVID-19). Using effective S-protein inhibitors may reduce the virulence of the virus. Molecular docking was performed to evaluate the binding affinity of 97 phenolic compounds (phenolics) with the SARS-CoV-2 S-protein receptor-binding domain (RBD). Molecular dynamics (MD) simulation was carried out to assess the stability of interactions between top-ranked compounds and S-protein RBD. Pharmacokinetics and toxicity of top-ranked inhibitors were also studied. Furthermore, the essential residues involved in ligand binding, based on the degree of each amino acid in the ligand-amino acid interaction (LAI) network for S-protein, were identified. Molecular docking and MD simulations were performed utilizing the AutoDock and Discovery Studio Client version, respectively. The LAI network was analyzed using the Cytoscape software. Pharmacokinetics and toxicity of top-ranked compounds were studied using bioinformatics webservers. It was estimated that nine of the studied phenolics can bind to the SARS-CoV-2 S-protein at the nanomolar scale with a considerable estimated energy of binding ( $\Delta G_{\text{binding}} < -10$  kcal/mol). Eight of them revealed stable docked pose after MD simulation. The results of the present study may be useful in the prevention and therapeutic perspectives of COVID-19. However, further *in vitro* and *in vivo* validation tests are required in the future.

**Keywords:** COVID-19; drug; molecular docking; molecular dynamics; SARS-CoV-2; spike protein

\*Corresponding author. E-mail: amir.007.taherkhani@gmail.com, amir\_007\_taherkhani@yahoo.com, a.taherkhani@umsha.ac.ir; phone: +98-9183145963.

**Abbreviations:** ACE2 = angiotensin-converting enzyme 2; ADME = absorption, distribution, metabolism, and excretion; BBB = blood-brain barrier; COVID-19 = coronavirus disease 2019; EM = energy minimization; GI = gastrointestinal absorption; HSV-1 = herpes simplex virus-1; IC<sub>50</sub> = half-maximal inhibitory concentration; Ki = inhibition constant; LAI = ligand-amino acid interaction; MD = molecular dynamics; P-gp = P-glycoprotein; RBD = receptor-binding domain; SARS-CoV-2 = severe acute respiratory syndrome coronavirus 2.

### Introduction

A new coronavirus has emerged in Wuhan city, Hubei province, China, on January 7, 2020. The International Committee on Taxonomy of Viruses named it severe acute respiratory syndrome coronavirus 2 (SARS-CoV-2), and the associated disorder was called coronavirus disease 2019 (COVID-19) by the World Health Organization (WHO). In addition, human-to-human transmission of the virus was early demonstrated in Guangdong, China (Chan *et al.*, 2020; Dai *et al.*, 2020; Wong *et al.*, 2020). Several clini-

cal symptoms have been reported for COVID-19, such as pneumonia (Shi *et al.*, 2020), fever (Chacón-Aguilar *et al.*, 2020), headache, nausea (Li and Huang, 2020), cough, fatigue (Wujtewicz *et al.*, 2020), and loss of taste and smell (Gautier and Ravussin, 2020).

It is necessary to discover effective vaccines and/or drugs to overcome this nasty pandemic (Gupta and Shah, 2021). Although vaccines provide long-term immunity against COVID-19 (Izda *et al.*, 2020), there are still certain limitations in this regard. According to previous reports, the effectiveness of vaccines depends on different factors including the patient's age (Campillo *et al.*, 2020), human genetics, and immune response, which varies in different ethnicities (Ozkan, 2020). Moreover, preparing vaccines in large enough amount for all recipients around the world is complicated and has not been achieved yet (Kumar *et al.*, 2021). Besides, the mRNA-based vaccines need to be kept at extremely cold temperatures (between  $-80^{\circ}\text{C}$  and  $-60^{\circ}\text{C}$ ), which is not easy to access in many health centers (Meo *et al.*, 2021). Thus, the availability of vaccines for COVID-19 is limited, and therefore, there is an urgent need to discover effective drugs against SARS-CoV-2 to reduce the mortality rate of patients affected with COVID-19 in a short-term treatment approach (Izda *et al.*, 2020, 2021).

SARS-CoV-2 infects host cells through an interaction between its surface glycoprotein, known as spike protein (S-protein), and the angiotensin-converting enzyme 2 (ACE2) located on the membrane of several organs cells such as lungs, kidney, heart, intestines, and arteries (Donoghue *et al.*, 2000; Hamming *et al.*, 2004; Xu *et al.*, 2020). Considering the essential role of S-protein in the pathogenesis, transmission, and the virulence of SARS-CoV-2, using potential S-protein inhibitors may reduce COVID-19 mortality and morbidity (Hall and Ji, 2020). Thus, S-protein inhibitors may be considered for therapeutic goals in the future. In the present study, *in silico* virtual screen approaches were performed, including molecular docking and molecular dynamics (MD) simulations, to estimate the binding affinity of 97 herbal phenolic compounds (phenolics) to the receptor-binding domain (RBD) of S-protein. AutoDock software was used to perform molecular docking analysis as one of the fastest methods for drug discovery (Huang and Zou, 2010).

Phenolics are natural antioxidants having one or more aromatic rings with at least one hydroxyl group. They are mostly found in fruits, vegetables, legumes, cereals, nuts, medicinal plants, spices, and several beverages such as tea and grape juice (Escarpa and Gonzalez, 2001; Palma *et al.*, 2002; Naczka and Shahidi, 2006; Garcia-Salas *et al.*, 2010; Guajardo-Flores *et al.*, 2013; Ramírez-Jiménez *et al.*, 2014; Wang *et al.*, 2015). Based on their basic structure, they are classified into several groups including simple phenolics ( $\text{C}_6$ ), benzoic acid ( $\text{C}_6\text{-C}_1$ ), acetophenones ( $\text{C}_6\text{-C}_2$ ),

cinnamic acid ( $\text{C}_6\text{-C}_3$ ), naphthoquinones ( $\text{C}_6\text{-C}_4$ ), xanthenes ( $\text{C}_6\text{-C}_1\text{-C}_6$ ), stilbenes ( $\text{C}_6\text{-C}_2\text{-C}_6$ ), flavonoids ( $\text{C}_6\text{-C}_3\text{-C}_6$ ), lignans and neolignans ( $\text{C}_6\text{-C}_3$ )<sub>2</sub>, hydrolyzable tannins ( $\text{C}_6\text{-C}_1$ )<sub>n</sub>, and lignins ( $\text{C}_6\text{-C}_3$ )<sub>n</sub> (Garcia-Salas *et al.*, 2010). Many beneficial functions have been reported for phenolics, such as antibacterial, anti-inflammatory, and antimutagenic activities (Garcia-Salas *et al.*, 2010; Saranraj *et al.*, 2019). Numerous studies have been published on the antiviral properties of several phenolic compounds. (Herrmann and Kucera, 1967; Serkedzhieva *et al.*, 1986a,b; Serkedzhieva and Manolova, 1988; Abou-Karam and Shier, 1992; Nagai *et al.*, 1995; Semple *et al.*, 1999; Gonçalves *et al.*, 2001; Likhitwitayawuid *et al.*, 2005; Sokmen *et al.*, 2005; Cai *et al.*, 2006; Dhiman, 2011; Xiong *et al.*, 2012; Pang *et al.*, 2014; Malik *et al.*, 2016; Ma *et al.*, 2018; Min *et al.*, 2018; Seong *et al.*, 2018; Nishide *et al.*, 2019; Ikeda *et al.*, 2020; Ulomskiy *et al.*, 2020; Yin *et al.*, 2014). Moreover, the antiviral activity of several flavonoids, the most abundant subclass of phenolics, has been experimentally confirmed against coronavirus infection (Russo *et al.*, 2020). Therefore, we hypothesized that phenolics may exhibit inhibitory effects against the SARS-CoV-2 S-protein. To examine this hypothesis, we designed a study based on molecular docking analysis to evaluate the binding affinity of several phenolic compounds to the SARS-CoV-2 S-protein RBD.

A total of nine studied phenolics were found to be top-ranked inhibitors of S-protein concerning their salient estimated energy of binding ( $\Delta G_{\text{binding}} < -10$  kcal/mol) and inhibition constant ( $K_i$ ). The  $K_i$  value of these compounds was estimated at the nanomolar scale (nM). Eight of the compounds showed a stable connection with the S-protein RBD after MD simulations and were considered as potentially effective S-protein inhibitors. The pharmacokinetic profiles and toxicological properties of top-ranked phenolics were also studied using bioinformatics web tools.

## Materials and Methods

**S-protein RBD and ligand structure preparation.** The 3-D structure of S-protein RBD was obtained from the Research Collaboratory for Structural Bioinformatics database (<https://www.rcsb.org>) (PDB ID: 6MOJ) as a Protein Data Bank (PDB) file by the criteria of x-ray resolution = 2.45 Å (Lan *et al.*, 2020). Chain E and chain A in the 6MOJ file corresponded to the S-protein RBD and ACE2, respectively. The chain E, with the length of 194 residues was selected for the molecular docking operation. Energy minimization (EM) of the S-protein RBD was performed using Swiss-PDB viewer version 4.1.0 (<http://www.expasy.org/spdbv>) before the molecular docking procedure. The EM was performed by using the GROMOS96 force-Field. In this approach, all calculations are made in a vacuum status,

with no reaction field (Artimo *et al.*, 2012). A total of 97 phenolics were considered as candidates for interaction with the SARS-CoV-2 S-protein. Several factors were considered for selecting a set of 97 phenolics in this study. Being herbal was the most important criteria for ligand selection due to their low toxicity, as well as their availability (Benalla *et al.*, 2010). In addition, having high molecular mass, as well as demonstrated antiviral property in previous studies were also considered as the next important features of the components. We hypothesized that high molecular mass allows the compound to cover the surface of the S-protein RBD as much as possible. Of note, we did not choose all the ligands of high molecular mass compounds with a known antiviral property showed in previous studies, because then we would lose many phenolics. However, several studied phenolics had a high molecular mass such as vitisin A (PubChem ID: 16131430), vitisin A (PubChem ID: 135430431; pyranoanthocyanin) and theaflavins. Among 97 studied compounds, a total of 29 plant-based ligands were selected from our previous studies, which were performed to examine their binding affinity to matrix metalloproteinase 8 (MMP-8) (Taherkhani *et al.*, 2021) and MMP-13 (Taherkhani *et al.*, 2020). The others were selected by text mining.

The 3-D Structures of all compounds (ligands) were obtained as a Structure Data File (SDF) file from the PubChem database (<https://pubchem.ncbi.nlm.nih.gov>). After that, the SDF formats were turned into the PDB file, using the cactus webserver (<http://cactus.nci.nih.gov/chemical/structure>). All ligands were structurally and geometrically optimized through EM, utilizing HyperChem version 08.0.10 software. Moreover, ChemDraw Ultra version 12.0.2.1076 (<http://www.cambridgesoft.com>) was used to draw the two-dimensional structures of top-ranked inhibitors.

**Molecular docking and molecular dynamics simulation.** In the present study, the computational analyses were done using a windows-based operating system. The characteristics of the system were as follows: Installed memory, 32 GB; Processor, Intel Core i7; System type, 64-bit. Molecular docking studies were implemented utilizing the AutoDock version 4.0 (<http://autodock.scripps.edu>). It is noteworthy that the AutoDock software uses the Lamarckian Genetic algorithm to predict the conformation of small molecules attached to the receptor. Moreover, AutoDock calculates the estimated free energy of binding ( $\Delta G_{\text{binding}}$ ) through the following formulas (Morris *et al.*, 1998; Huey *et al.*, 2007; Huey and Morris, 2008; Liu *et al.*, 2016; Jayaraj *et al.*, 2021):

$$\Delta G_{\text{binding}} = G_{\text{complex}} - (G_{\text{protein}} + G_{\text{ligand}})$$

$$\Delta G_{\text{binding}} = \text{Intermolecular Energy} + \text{Total Internal Energy} + \text{Torsional Free Energy} - \text{Unbound System's Energy}$$

According to Lan *et al.* (2020), a total of 17 residues of the SARS-CoV-2 RBD are bound to 20 amino acids of ACE2. The interacting amino acids in the RBD included K417, G446, Y449, Y453, L455, F456, A475, F486, N487, Y489, Q493, G496, Q498, T500, N501,

G502, and Y505. In the AutoDock software, the grid box settings were as follows: spacing, 0.375 Å; X-dimension, 48; Y-dimension, 100; Z-dimension, 52; X-center, -36.669; Y-center, 29.44; Z-center, 4.183. In addition to the setting options in AutoDock, the number of ligand conformations was set as 50. For each of the top-ranked inhibitors, the conformation with the lowest  $\Delta G_{\text{binding}}$  involved in a cluster with the highest frequency of models using a root-mean-square deviation (RMSD)-tolerance of 2.0 Å was selected to create the docked protein-ligand complex. To study the stability of interactions between top-ranked phenolics and S-protein RBD, MD simulations were implemented in a period of 1 nanosecond (ns) using Discovery Studio Client version 16.1.0.15350. The MD simulation advanced settings were as follows: solvation model, explicit periodic boundary; cell shape, orthorhombic; minimum distance from the boundary, 10 Å; solvent, water; target temperature, 310 K; force field, CHARMM; and time step, 2 fs. Moreover, BIOVIA Discovery Studio Visualizer version 19.1.0.18287 was used to demonstrate interaction modes between top-ranked inhibitors and residues within the S-protein RBD, as well as their three-dimensional docked pose before and after MD simulations.

**Pharmacokinetic and toxicological properties.** The pharmacokinetic features of the top-ranked inhibitors were predicted using the SwissADME web tool (<http://www.swissadme.ch/>). These characteristics included absorption, distribution, metabolism, and excretion (ADME) of the compounds. Also, the PreADMET (<https://preadmet.bmdrc.kr/>) web-tool was used to evaluate the carcinogenicity of top-ranked phenolics in mouse and rat models, besides estimating the *in vitro* human etheragogo related gene (hERG) inhibition.

**LAI network analysis.** In the present study, a set of amino acids connected to each of the inhibitors with a  $K_i$  value at the nanomolar scale were identified from post-docking analysis using the BIOVIA Discovery Studio Visualizer 19.1.0.18287. Accordingly, a list of phenolics and their interacted residues was imported into the Cytoscape (3.7.2; [www.cytoscape.org](http://www.cytoscape.org)) to build an LAI network. The network was analyzed using the network analyzer tool to calculate the degree of all amino acids in the network.

## Results and Discussion

### *Molecular docking and dynamics between the S-protein RBD and phenolic compounds*

In the present study, computational protein-ligand docking was performed to evaluate the binding affinity between the RBD of S-protein in SARS-CoV-2 and 97 phenolics. The docking results of all tested compounds in this study are presented in Supplementary Table 1. According to the results, a total of nine compounds with a  $\Delta G_{\text{binding}}$  less than -10 kcal/mol and a  $K_i$  value at the nM scale were

**Table 1. Details of binding energies between SARS-CoV-2 spike protein RBD and top nine phenolic inhibitors**

Ligand name	Final intermolecular energy (kcal/mol)	Final total internal energy (kcal/mol)	Torsional free energy (kcal/mol)	Unbound system's energy (kcal/mol)	Estimated free energy of binding (kcal/mol)
Vitisin A	-10.53	-10.42	+5.37	-3.59	-11.99
Theaflavin-3,3'-digallate	-11.56	-9.20	+6.26	-3.23	-11.26
Vitisin A (pyranoanthocyanin)	-7.91	-7.32	+4.18	-0.09	-10.95
Vicenin-2	-9.82	-8.09	+4.77	-2.40	-10.73
Hesperidin	-8.70	-8.17	+4.47	-1.95	-10.45
Astilbin	-9.43	-5.23	+2.98	-1.30	-10.38
Rutin	-7.23	-9.74	+4.77	-2.10	-10.1
Theaflavin	-9.12	-5.35	+3.28	-1.11	-10.09
Amentoflavone	-9.91	-4.21	+2.68	-1.38	-10.05

SARS-CoV-2, severe acute respiratory syndrome coronavirus 2; RBD, receptor binding domain.

identified; these ligands were considered as top-ranked phenolics for inhibition of S-protein. The range of  $\Delta G_{\text{binding}}$  for the top nine S-protein inhibitors was determined between -11.99 and -10.05 kcal/mol for vitisin A (PubChem ID: 16131430) and amentoflavone (PubChem ID: 5281600), respectively. Therefore, it was estimated that all of the top-ranked inhibitors could strongly bind to the S-protein RBD. The details of docking results related to each of the top nine inhibitors analyzed in the current study are presented in Table 1. The details of interaction modes between each of the top nine phenolics and residues within the S-protein RBD, before and after MD simulations are presented in Table 2. Of note, all hydrogen bonds with a distance longer than 5 Å were not considered significant.

#### *Pharmacokinetic and toxicological properties of top-ranked inhibitors*

The *in silico* prediction approach was used to evaluate the ADME and toxicity of the top-ranked S-protein inhibitors, since traditional methods are time-consuming and costly (Yamashita & Hashida, 2004; Moda, 2007; Buzzi, 2007; Afonso, 2008; Silva, 2008; de Amorim *et al.*, 2018). Several pharmacokinetic properties were studied using Swiss ADME, including gastrointestinal (GI) absorption, blood-brain barrier (BBB) permeability, P-gp (P-glycoprotein) substrate, and cytochrome P-450 inhibition. The possible inhibition of human cardiac potassium channel hERG, besides carcinogenicity of the compounds in mice and rats, were considered as toxicological properties of the top nine inhibitors. According to the results, it was estimated that vicenin-2 and rutin have lower toxicity effects than the other top inhibitors. The ADME and toxicity results are presented in Table 3.

#### *LAI network analysis*

The LAI network contained 126 interactions between 44 nodes. The nodes included 23 compounds with a  $K_i$  value at the nM scale, besides 21 interacting amino acids (Fig. 1). NetworkAnalyzer defined the degree of all amino acids in the network. Tyr453 was found to be the most interacting residue within the S-protein RBD (Fig. 2).

In the present study, virtual screening approaches were performed using the AutoDock tool and Discovery Studio Client to identify effective plant-based phenolics for inhibiting the S-protein located at the surface of SARS-CoV-2. To the best of our knowledge, the present study is the first, in which an LAI network associated with the S-protein amino acids was built to determine the most essential amino acids involved in the ligand binding.

According to the docking results, vitisin A (PubChem ID, 16131430) illustrated the highest binding affinity to S-protein with the  $\Delta G_{\text{binding}}$  and  $K_i$  value of -11.99 kcal/mol and 1.62 nM, respectively. The next top S-protein inhibitors ranked as follows: theaflavin-3,3'-digallate, pyranoanthocyanidin (vitisin A, ID = 135430431), vicenin-2, hesperidin, astilbin, rutin, theaflavin, and amentoflavone. The two-dimensional structures and sources of each of the top nine inhibitors are presented in Supplementary Table 2.

Hall *et al.* (2020) performed a molecular docking study of various available anti-viral medications against the S-protein and main protease of SARS-CoV-2, known as 3CL, using Schrödinger® docking suits (Schrödinger Maestro, New York, NY, USA. Version 11.9.011, MMshare Version 4.5.011, Release 2019-1, Platform Windows-x64). According to the results of the study by Hall *et al.* (Hall & Ji, 2020), Coenzyme A and Flavin Adenine Dinucleotide (also called adeflavin) revealed the best results for S-protein inhibi-

**Table 2. Molecular interactions between the top nine phenolic inhibitors and residues incorporated in the receptor binding domain of spike protein before molecular dynamics and after molecular dynamics simulations**

Ligand name	Hydrogen bond (distance Å)	Hydrophobic interaction (distance Å)	Electrostatic (distance Å)	Miscellaneous (distance Å)	Unfavorable (distance Å)
Vitisin A (before MD)	Arg403 (4.41 non-classical); Gly496 (2.91 classical); Ser494* (3.54 classical)	Phe456 (6.63); Tyr489 (5.40); Leu455* (5.85); Tyr449 (6.77, 7.17)	Arg403 (7.07)	NA	Phe490 (4.37)
Vitisin A (after MD)	Ser494 (3.37 classical); Gln493 (3.80 non-classical); Gly496 (3.62 non-classical)	Leu455 (7.01)	NA	NA	NA
Theaflavin-3,3'-digallate (before MD)	Tyr453 (4.58 classical)	Tyr505 (3.82, 4.71)	Arg403 (6.26)	Gln498 (4.99)	Ser494 (4.82)
Theaflavin-3,3'-digallate (after MD)	Asn501 (3.22 non-classical)	NA	NA	NA	NA
Vitisin A: pyranoanthocyanin (before MD)	Gly496 (3.50 non-classical); Arg403 (4.92 classical)	NA	NA	NA	NA
Vitisin A: pyranoanthocyanin (after MD)	Tyr505 (4.77 classical); Gly496 (3.16 classical); Arg403 (4.33 non-classical); Ser494 (3.73 classical, 4.97 non-classical); Gln493 (3.31 classical)	Tyr605 (6.19)	NA	NA	NA
Vicenin-2 (before MD)	Glu484* (4.76 classical, 4.97 classical); Ser494* (2.12 classical, 3.13 classical); Gly496 (2.21 classical)	NA	NA	NA	Phe490* (4.23, 5.78)
Vicenin-2 (after MD)	Glu484 (4.90 classical); Gln493 (3.88 classical, 4.14 classical); Ser494 (2.90 classical)	NA	NA	NA	Phe490* (4.90)
Hesperidin (before MD)	Gln493* (4.28 classical); Glu484 (4.28 classical, 4.62 classical)	Gln493 (3.95)	NA	NA	NA
Hesperidin (after MD)	Gln493 (4.70 classical); Tyr489 (4.57 non-classical)	NA	NA	NA	NA
Astilbin (before MD)	Glu484* (4.36 classical); Ser494 (3.18 classical, 3.96 classical); Tyr453 (4.63 classical)	NA	NA	NA	Phe490 (5.29)
Astilbin (after MD)	Glu484 (4.10 classical); Thr470 (4.82 classical, 3.67 classical);	Phe490 (3.65, 5.77)	NA	NA	NA
Rutin (before MD)	Gly496* (2.77 classical)	Tyr449 (6.45, 7.37); Tyr505 (5.94)	NA	NA	NA
Rutin (after MD)	Ser494 (3.80 classical); Tyr453 (4.84 classical); Tyr495 (3.70 non-classical); Gly496 (4.35 classical, 3.64 non-classical, 3.26 non-classical); Asn501 (3.68 classical)	Tyr495 (4.51); Phe497 (4.22)	NA	NA	NA
Theaflavin (before MD)	Leu492 (4.96 classical); Ser494* (2.84 classical)	Gln493 (4.09)	NA	NA	NA
Theaflavin (after MD)	Ser494 (4.35 classical); Tyr489 (4.08 non-classical)	Leu455 (6.01); Tyr473 (6.33)	NA	NA	NA
Amentoflavone (before MD)	Gly496 (3.40 non-classical); Gln493 (4.46 non-classical); Glu484* (4.73 classical)	Tyr449 (5.57); Gln493 (4.39)	NA	Ser494 (4.51)	NA
Amentoflavone (after MD)	Ser494 (3.38 classical); Glu484 (4.40 classical)	NA	NA	NA	NA

The asterisk (\*) symbol represents interactions that were conserved after MD simulations. MD, molecular dynamics.

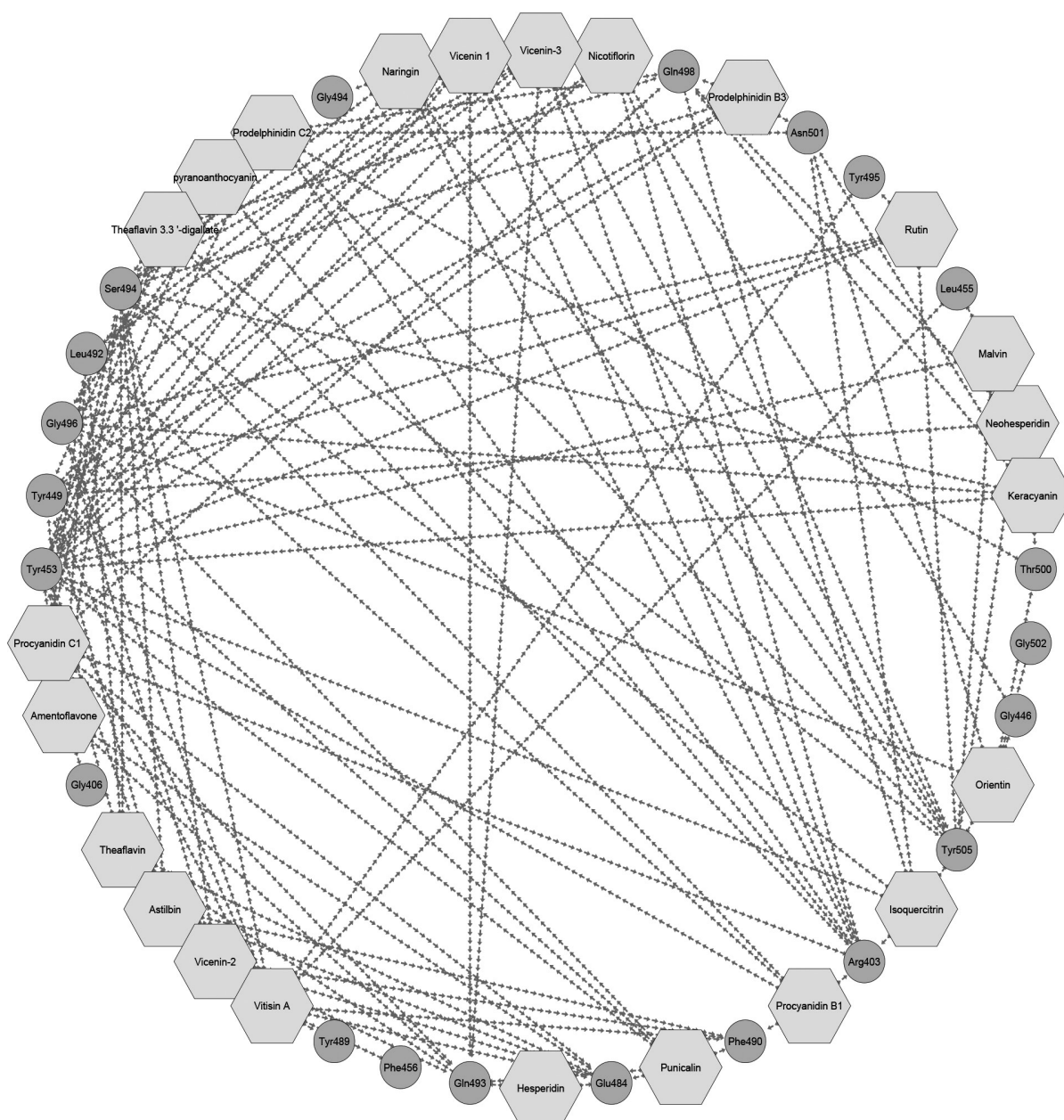


Fig. 1

**Ligand-amino acid interaction network of spike protein obtained from the docking results Hexagons represent phenolics, while circles reflect amino acids**

tion with docking scores of -11.55 and -11.089 kcal/mol, respectively. Moreover, Nicotine Adenine Dinucleotide (NADH) revealed a higher binding affinity to 3CL protease, with a docking score of -11.016 kcal/mol. Notably, Hall *et al.* (Hall and Ji, 2020) used the modeled structure of SARS-CoV-2 S-protein. The homology modeling was performed using the ModBase database (Pieper *et al.*, 2014).

Amin *et al.* (2020) performed a study to examine the binding affinity of hydroxychloroquine and chloroquine to SARS-CoV-2 S-protein. According to the results of the study by Amin *et al.* (2020), hydroxychloroquine and chloroquine demonstrated a potential inhibitory effect on S-protein with estimated binding energy of -7.28 and -6.30 kcal/mol, respectively. The authors suggested that

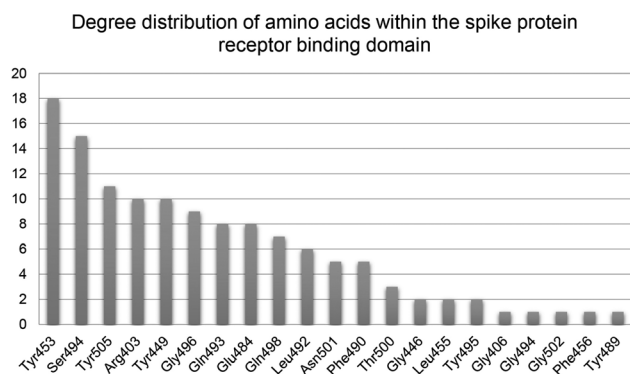


Fig. 2

## Degree diagram

The x-axis represents the name of amino acids within the spike protein receptor-binding domain. The y-axis represents the degree of each amino acid.

their results may provide insights into the molecular mechanism of hydroxychloroquine and chloroquine as potential treatments for COVID-19.

The antiviral activity of some of the top-ranked inhibitors in this study has been confirmed by previous experimental studies. Huang *et al.* (2008) identified vitisin A to be an anti-inflammatory agent that can inhibit influenza A (H1N1) virus-induced chemokine (C-C motif) ligand 5 production through down-regulating Akt- and STAT1-related signal pathways. Vitisin A is a natural tetramer phenol purified from *Vitis vinifera* roots with anticancer, antioxidant, and antiapoptotic properties (Sung *et al.*, 2009). According to the docking results of the present study, vitisin A (PubChem ID: 16131430), formed three hydrogen bonds with Arg403, Ser494, Gly496, five hydrophobic interactions with Tyr449, Leu455, Phe456, Tyr489, one electrostatic interaction with Arg403, and one unfavorable interaction with Phe490. Furthermore, the number of interactions between vitisin A and residues within the S-protein RBD decreased after MD simulation: it demonstrated three hydrogen and one hydrophobic interaction with Leu455, Gln493, Ser494, and Gly496.

de Oliveira *et al.* (2015) performed a study using plaque reduction assay, MTS assay, flow cytometry analysis, and confocal microscopy observations to evaluate the anti-herpes simplex virus-1 (HSV-1) activity of theaflavin polyphenols including theaflavin, theaflavin-3-monogallate, theaflavin-3'-monogallate, and theaflavin-3,3'-digallate. The authors reported that theaflavin polyphenol compounds exhibited an anti-HSV-1 effect in Vero and A549 cell lines. In addition to the results of the study by de Oliveira *et al.* (2015), treating the cell lines with theaflavin-3,3'-digallate 1 h before HSV-1 infection, inhibited more than

Table 3. Predicted pharmacokinetics and toxicological properties of the top nine phenolic inhibitors in this study

Ligand name	GI abs	BBB permeant	P-gp substrate	CYP1A2 inhibitor	CYP2C19 inhibitor	CYP2C9 inhibitor	CYP2D6 inhibitor	CYP3A4 inhibitor	hERG inhibitor	Carcinogenicity (mouse)	Carcinogenicity (Rat)
Vitisin A	Low	No	Yes	No	No	No	No	No	ambiguous	Negative	Positive
Theaflavin-3,3'-digallate	Low	No	Yes	No	No	Yes	No	No	ambiguous	Negative	Positive
Vitisin A (pyranoanthocyanin)	Low	No	No	No	No	No	No	Yes	high_risk	Positive	Negative
Vicenin-2	Low	No	No	No	No	No	No	No	ambiguous	Negative	Negative
Hesperidin	Low	No	Yes	No	No	No	No	No	high_risk	Negative	Negative
Astilbin	Low	No	Yes	No	No	No	No	No	high_risk	Negative	Negative
Rutin	Low	No	No	No	No	No	No	No	ambiguous	Negative	Negative
Theaflavin	Low	No	No	No	No	Yes	No	Yes	high_risk	Negative	Negative
Amentoflavone	Low	No	No	No	No	No	No	No	medium_risk	Negative	Positive

GI, gastrointestinal; abs, absorption; BBB, blood/brain barrier; P-gp, p-glycoprotein; CYP, cytochrome p-450; hERG, the human ether-a-go-go related gene.

99% of viral production at a concentration of 50  $\mu\text{M}$  (de Oliveira *et al.*, 2015). Moreover, Chen *et al.* (2005) reported a significant inhibitory effect of theaflavin-3,3'-digallate on SARS-CoV 3CL<sup>Pro</sup> with the half-maximal inhibitory concentration ( $\text{IC}_{50}$ ) = 9.5  $\mu\text{M}$ . According to the docking results of the present study, theaflavin-3,3'-digallate exhibited a high affinity of binding to SARS-CoV-2 S-protein with the  $\Delta G_{\text{binding}}$  and  $K_i$  value of -11.26 kcal/mol and 5.57 nM, respectively. Theaflavin-3,3'-digallate formed one hydrogen bond with Tyr453, besides two hydrophobic interactions with Tyr505, one electrostatic interaction with Arg403, one miscellaneous interaction with Gln498, and one unfavorable interaction with Ser494. The number of interactions between theaflavin-3,3'-digallate and residues within the S-protein RBD decreased after MD simulation: it only demonstrated one hydrogen bond with Asn501. Theaflavin-3,3'-digallate is a polyphenol compound found in black tea with antioxidant activity (Lin *et al.*, 1999).

Han *et al.* (2015) demonstrated that rutin and its several derivatives had anti-viral activity against tobacco mosaic virus and cucumber mosaic virus at the concentration of 500  $\mu\text{g}/\text{ml}$ . According to docking results of the present study, rutin revealed a high affinity of binding to SARS-CoV-2 S-protein with the  $\Delta G_{\text{binding}}$  and  $K_i$  value of -10.1 kcal/mol and 39.46 nM, respectively: it demonstrated one hydrogen bond with Gly496, and three hydrophobic interactions with Tyr449 and Tyr505. Moreover, the number of interactions between rutin and residues within the S-protein RBD increased after MD simulation: it demonstrated seven hydrogen and two hydrophobic interactions with Tyr453, Ser494, Tyr495, Gly496, Phe497, and Asn501. Rutin was found in various plants such as tea, apple, buckwheat, and passionflower (Ganeshpurkar and Saluja, 2017).

Ma *et al.* (2001) reported that amentoflavone had anti-respiratory syncytial virus activity with the  $\text{IC}_{50}$  = 5.5  $\mu\text{g}/\text{ml}$ . According to the docking results we estimated that amentoflavone can robustly bind to SARS-CoV-2 S-protein with the  $\Delta G_{\text{binding}}$  and  $K_i$  value of -10.05 kcal/mol and 42.89 nM, respectively: it performed three hydrogen bonds with Glu484, Gln493, Gly496, two hydrophobic interactions with Tyr449, Gln493, and one miscellaneous interaction with Ser494. After the MD simulation, amentoflavone formed two hydrogen bonds with Glu484 and Ser494 within the S-protein RBD. Several pharmacological activities have been reported for amentoflavone, including antioxidant (Arwa *et al.*, 2015), anti-inflammatory (Abdallah *et al.*, 2015), anticancer (Ndongo *et al.*, 2015), antiviral (Coulerie *et al.*, 2013), and anti-*Candida Albicans* effects (Hwang *et al.*, 2012). *Calophyllaceae*, *Clusiaceae*, *Cupressaceae*, *Euphorbiaceae* are rich sources of amentoflavone (Yu *et al.*, 2017).

It is noteworthy that in a previous study, Taherkhani *et al.* (2021) reported considerable binding affinity of rutin

and amentoflavone with the MMP-8 which is upregulated in several disorders such as dental caries (Imran *et al.*, 2019), periodontal disease (de de Moraes *et al.*, 2018), acute/chronic inflammation (Van Lint and Libert, 2006), animals with experimental autoimmune encephalomyelitis (Armstrong and Ernst, 1999), humans and animals with experimental bacterial meningitis (Leib *et al.*, 2000; Leppert *et al.*, 2000), and cancer progression and invasion (Moilanen *et al.*, 2002).

Kim *et al.* (2020) performed a study to examine the antiviral activity of several chemical compounds extracted from *Elaeocarpus sylvestris* against varicella-zoster virus (VZV) and human cytomegalovirus (HCMV) production *in vitro*. According to the results of the study by Kim *et al.* (Kim *et al.*, 2020), quercetin and isoquercitrin demonstrated antiviral activity against both VZV and HCMV, besides not having any significant side effects. According to the results of our study, it was estimated that isoquercitrin has a high affinity of binding to S-protein RBD with the  $\Delta G_{\text{binding}}$  and  $K_i$  value of -8.52 kcal/mol and 567.08 nM, respectively.

It is noteworthy that among all interaction modes between ligands and proteins, salt-bridges,  $\pi$  -  $\pi$  stack pairing, and  $\pi$ -charge pairing are the most stabilizing hydrogen, hydrophobic, and electrostatic interactions, respectively (Muthusamy *et al.*, 2016). According to the results, the following stabilizing interactions were observed before MD simulations: vitisin A (PubChem ID: 16131430) demonstrated four  $\pi$  -  $\pi$  stack pairing interactions with Tyr449 (6.77 Å, 7.17 Å), Phe456 (6.63 Å), and Tyr489 (5.40 Å). Furthermore, vitisin A formed a  $\pi$ -charge pairing interaction with Arg403 (7.07 Å). Theaflavin-3,3'-digallate showed a  $\pi$ -charge pairing interaction with Arg403 (6.26 Å). Rutin illustrated two  $\pi$  -  $\pi$  stack pairing interactions with Tyr449 (6.45 Å, 7.37 Å). Amentoflavone formed a  $\pi$  -  $\pi$  stack pairing interaction with Tyr449 (5.57 Å). Furthermore, the following important interactions were noticed after MD simulations: vitisin A (PubChem ID: 135430431; pyranoanthocyanin) demonstrated a  $\pi$  -  $\pi$  stack pairing interaction with Tyr505 (6.19 Å). Astilbin formed a  $\pi$  -  $\pi$  stack pairing interaction with Phe490 (5.77 Å). The two-dimensional images of interaction modes between the top nine inhibitors in this study and residues within the S-protein RBD before and after MD simulations are shown in Fig. 3.

Among the top 9 inhibitors which were ranked based on their  $\Delta G_{\text{binding}}$ , we found that the docked pose between theaflavin-3,3'-digallate and the S-protein RBD is not very stable due to the absence of any stable interaction between theaflavin-3,3'-digallate and the residues within the S-protein RBD. Moreover, only one interaction (a non-classical hydrogen bond) was found between theaflavin-3,3'-digallate and S-protein RBD after MD simulation, and therefore, this compound could not be considered





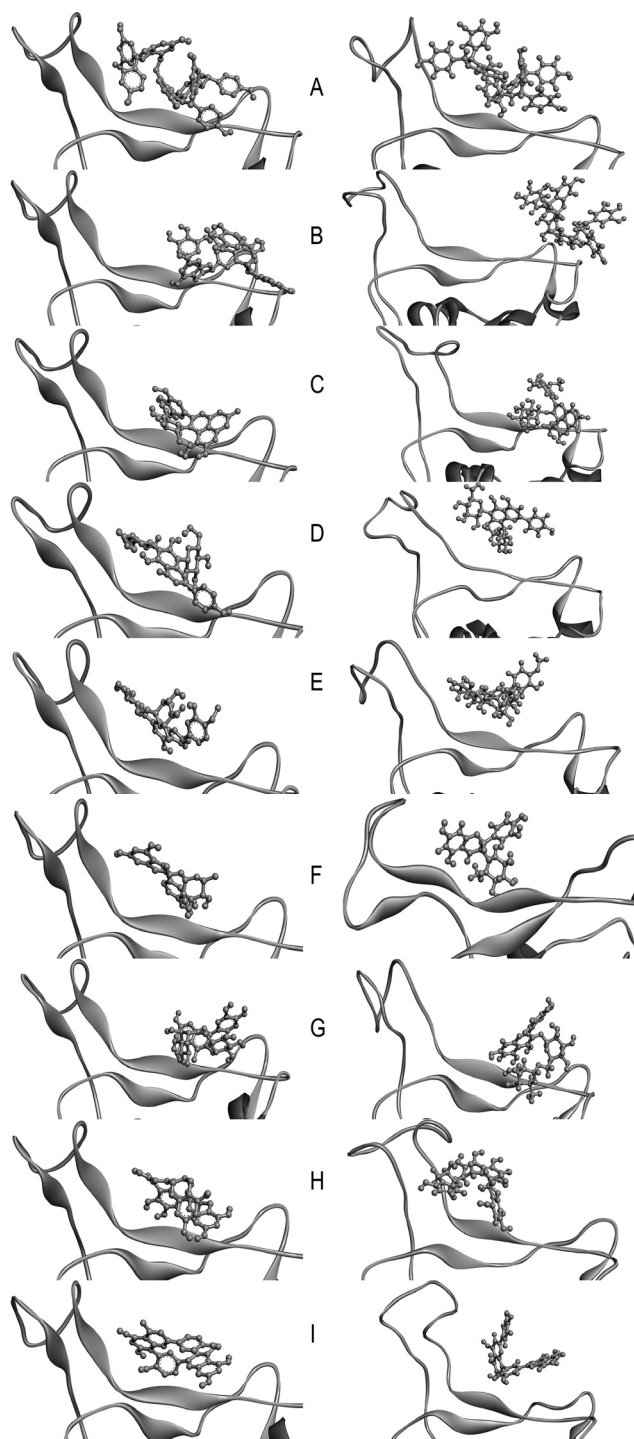


**Fig. 4**

**Docked pose: left, before MD simulations, and right, after MD simulations for (A) vitisin A (PubChem ID: 16131430), (B) theaflavin-3,3'-digallate, (C) vitisin A (PubChem ID: 135430431; pyranoanthocyanin), (D) vicenin 2, (E) hesperidin, (F) astilbin, (G) rutin, (H) theaflavin, and (I) amentoflavone within the spike protein receptor-binding domain**  
MD, molecular dynamics.

fective inhibitors of SARS-CoV-2 S-protein and may block the connection between S-protein and ACE2, leading to disruption of the viral life cycle. Fig. 4 demonstrates the three-dimensional docked pose of top-ranked inhibitors before and after MD simulations.

Moreover, structural analysis revealed that the condensation, polymerization, and glycosylation of phenolics resulted in lower estimated  $\Delta G_{\text{binding}}$ . Accordingly, the following points are noteworthy:

- In the case of condensation: theaflavin-3,3'-digallate is formed from the condensation of a flavan-3-ols (e.g., catechin and epicatechin) and gallate residue. According to the results of this study, theaflavin-3,3'-digallate bonded with S-protein RBD more tightly than catechin and epicatechin did.
- In the case of polymerization: vitisin A is tetramer resveratrol and revealed a higher binding affinity to S-protein RBD as compared with the resveratrol.
- In the case of glycosylation: vicenin 1, vicenin 1, vicenin 2, and vicenin 3, which are diglycosylated apigenin compounds, demonstrated a better interaction with S-protein RBD compared with the apigenin.

We had a certain limitation in our study. MD simulation is well-known as a time-exhausting process (Shen and Yang, 2018). We performed MD simulation for nine of the ligand-protein complexes by using only a windows-based operating system due to the lack of a supercomputer for the research team, which took several weeks to carry out MD simulations. We believe that calculating MD simulation in greater time scales leads to more authentic results, although it needs more robust processors.

## Conclusions

In conclusion, we aimed to identify plant-based phenolics for possible SARS-CoV-2 S-protein inhibition. Based on the results of the docking score, the range of  $\Delta G_{\text{binding}}$  for the top nine inhibitors varied from -11.99 to -10.05 kcal/mol. After MD simulations, it was revealed that the docked pose of vitisin A (PubChem ID: 16131430), vitisin A (PubChem ID: 135430431; pyranoanthocyanin), vicenin 2, hesperidin, astilbin, rutin, theaflavin, and amentoflavone is stable, suggesting that these compounds can tightly bind to the SARS-CoV-2 S-protein which is essential for entering the virus into the host cells. Therefore, it may be hypothesized that these phenolics are effective in combating the SARS-CoV-2 life cycle and may be considered as drug candidates for COVID-19. In addition, it was demonstrated that Tyr453 was the most potent residue in the inhibition of SARS-CoV-2 S-protein. Accordingly, computational drug design and discovery could focus on the blocking of Tyr453 to diminish the transmission

of SARS-CoV-2. Considering the sources of the top-ranked compounds in this study, we hypothesize that the daily intake of several dietary plants and vegetables such as citrus fruits, black tea, and red grape may reduce the virulence of COVID-19. Although our findings need validation using wet-lab experiments, they provided knowledge about the inhibition of SARS-CoV-2 S-protein using phenolic compounds and could be used in providing study designs in the future.

**Acknowledgments.** The authors would like to appreciate the Deputy of Research and Technology, Medicinal Plants and Natural Product Research Center, and Research Center for Molecular Medicine, Hamadan University of Medical Sciences, Hamadan - Iran, for their supports. This research received no specific grant from any funding agency in the public, commercial, or not-for-profit sectors. Ethics No. IR.UMSHA.REC-1399.348.

**Supplementary information** is available in the online version of the paper.

## References

- Abdallah HM, Almowallad FM, Esmat A, Shehata IA, Abdel-Sattar EA (2015): Anti-inflammatory activity of flavonoids from *Chrozophora tinctoria*. *Phytochem. Lett.* 13, 74–80. <https://doi.org/10.1016/j.phytol.2015.05.008>
- Abou-Karam M, Shier WT (1992): Isolation and characterization of an antiviral flavonoid from *Waldsteinia fragarioides*. *J. Nat. Prod.* 55, 1525–1527. <https://doi.org/10.1021/np50088a022>
- Afonso IF (2008): Modelagem Molecular e Avaliação da Relação Estrutura-Atividade Acoplados a Estudos Farmacocinéticos e Toxicológicos in silico de Derivados Heterocíclicos com Atividade Antimicrobiana: dissertation. Rio de Janeiro, Brazil: Universidade Federal do Rio de Janeiro.
- Amin M, Abbas G (2020): Docking study of Chloroquine and Hydroxychloroquine interaction with SARS-CoV-2 spike glycoprotein-An in silico insight into the comparative efficacy of repurposing antiviral drugs. *J. Biomol. Struct. Dyn.* 1–13.
- Armstrong N, Ernst E (1999). The treatment of eczema with Chinese herbs: a systematic review of randomized clinical trials. *Br. J. Clin. Pharmacol.* 48(2), 262. <https://doi.org/10.1046/j.1365-2125.1999.00004.x>
- Artimo P, Jonnalagedda M, Arnold K, Baratin D, Csardi G, De Castro E, Duvaud S, Flegel V, Fortier A, Gasteiger E (2012): ExPASy: SIB bioinformatics resource portal. *Nucleic Acids Res.* 40(W1), W597–W603. <https://doi.org/10.1093/nar/gks400>
- Arwa PS, Zeraik ML, Ximenes VF, da Fonseca LM, da Silva Bolzani V, Silva DHS (2015): Redox-active biflavonoids from *Garcinia brasiliensis* as inhibitors of neutrophil oxidative burst and human erythrocyte membrane damage. *J. Ethnopharmacol.* 174, 410–418. <https://doi.org/10.1016/j.jep.2015.08.041>
- Benalla W, Bellahcen S, Bnouham M (2010): Antidiabetic medicinal plants as a source of alpha glucosidase inhibitors. *Curr. Diabetes Rev.* 6(4), 247–254. <https://doi.org/10.2174/157339910791658826>
- Buzzi FdC (2007): Síntese de novas moléculas com potencial terapêutico: imidas cíclicas, chalconas e compostos relacionados. Santa Catarina: Federal University of Santa Catarina.
- Cai SQ, Wang R, Yang X, Shang M, Ma C, Shoyama Y (2006): Antiviral flavonoid-type C-glycosides from the flowers of *Trollius chinensis*. *Chem. Biodivers.* 3(3), 343–348. <https://doi.org/10.1002/cbdv.200690037>
- Campillo NE, Jimenez, M, Canelles M (2020): COVID-19 vaccine race: analysis of age-dependent immune responses against SARS-CoV-2 indicates that more than just one strategy may be needed. *Curr. Med. Chem.* <https://doi.org/10.2174/0929867327666201027153123>
- Chacón-Aguilar, R, Osorio-Cámara J M, Sanjurjo-Jimenez I, González-González C, López-Carnero J, Pérez-Moneo-Agapito B (2020): COVID-19: Fever syndrome and neurological symptoms in a neonate. *An Pediatr (Engl Ed)*. <https://doi.org/10.1016/j.anpede.2020.04.001>
- Chan JFW, Yuan S, Kok K-H, To KK-W, Chu H, Yang J, Xing F, Liu J, Yip CC-Y, Poon RW-S (2020): A familial cluster of pneumonia associated with the 2019 novel coronavirus indicating person-to-person transmission: a study of a family cluster. *Lancet* 395(10223), 514–523. [https://doi.org/10.1016/S0140-6736\(20\)30154-9](https://doi.org/10.1016/S0140-6736(20)30154-9)
- Chen CN, Lin CP, Huang KK, Chen WC, Hsieh HP, Liang PH, Hsu JT (2005): Inhibition of SARS-CoV 3C-like Protease Activity by Theaflavin-3,3'-digallate (TF3). *Evid. Based. Complement Alternat. Med.* 2(2), 209–215. <https://doi.org/10.1093/ecam/neh081>
- Coulerie P, Nour M, Maciuk A, Eydoux C, Guillemot J-C, Lebouvier N, Hnawia E, Leblanc, K, Lewin G, Canard B (2013): Structure-activity relationship study of biflavonoids on the Dengue virus polymerase DENV-NS5 RdRp. *Planta Med.* 79(14), 1313–1318. <https://doi.org/10.1055/s-0033-1350672>
- Dai W, Zhang B, Su H, Li J, Zhao Y, Xie X, Jin Z, Liu F, Li C, Li, Y (2020): Structure-based design of antiviral drug candidates targeting the SARS-CoV-2 main protease. *Science* 368, 1331–1335. <https://doi.org/10.1126/science.abb4489>
- de Amorim AL, de Lima AVM, do Rosário, AC, dos Santos Souza ÉT, Ferreira JV, da Silva Hage-Melim LI (2018): Molecular modeling of inhibitors against fructose biphosphate aldolase from *Candida albicans*. In *Silico Pharmacol.* 6(1), 2. <https://doi.org/10.1007/s40203-018-0040-x>
- de de Moraes EF, Dantas AN, Pinheiro JC, Leite RB, Barboza CAG, de Vasconcelos Gurgel BC, de Almeida Freitas R (2018): Matrix metalloproteinase-8 analysis in patients with periodontal disease with prediabetes or type 2 diabetes mellitus: A systematic review. *Arch. Oral Biol.* 87, 43–51. <https://doi.org/10.1016/j.archoralbio.2017.12.008>

- de Oliveira A, Prince D, Lo CY, Lee LH, Chu, TC (2015): Antiviral activity of theaflavin digallate against herpes simplex virus type 1. *Antiviral Res.* 118, 56–67. <https://doi.org/10.1016/j.antiviral.2015.03.009>
- Dhiman RK (2011): The Green Tea Polyphenol, Epigallocatechin-3-Gallate (EGCG)—One Step Forward in Antiviral Therapy Against Hepatitis C Virus. *J. Clin. Exp. Hepatol.* 1(3), 159–160. [https://doi.org/10.1016/S0973-6883\(11\)60232-6](https://doi.org/10.1016/S0973-6883(11)60232-6)
- Donoghue M, Hsieh F, Baronas E, Godbout K, Gosselin M, Stagliano N, Donovan M, Woolf B, Robison K, Jeyaseelan R, Breitbart RE, Acton S (2000): A novel angiotensin-converting enzyme-related carboxypeptidase (ACE2) converts angiotensin I to angiotensin 1-9. *Circ. Res.* 87(5), E1–9. <https://doi.org/10.1161/01.RES.87.5.e1>
- Escarpa A, Gonzalez M (2001): An overview of analytical chemistry of phenolic compounds in foods. *Crit. Rev. Anal. Chem.* 31(2), 57–139. <https://doi.org/10.1080/20014091076695>
- Ganeshpurkar A, Saluja AK (2017): The Pharmacological Potential of Rutin. *Saudi Pharm. J.* 25(2), 149–164. <https://doi.org/10.1016/j.jsps.2016.04.025>
- Garcia-Salas P, Morales-Soto A, Segura-Carretero A, Fernández-Gutiérrez A (2010): Phenolic-compound-extraction systems for fruit and vegetable samples. *Molecules* 15(12), 8813–8826. <https://doi.org/10.3390/molecules15128813>
- Gautier JF, Ravussin Y (2020): A New Symptom of COVID-19: Loss of Taste and Smell. *Obesity (Silver Spring)*. 28(5), 848. <https://doi.org/10.1002/oby.22809>
- Gonçalves JL, Leitão SG, Monache FD, Miranda MM, Santos MG, Romanos MT, Wigg MD (2001): In vitro antiviral effect of flavonoid-rich extracts of *Vitex polygama* (Verbenaceae) against acyclovir-resistant herpes simplex virus type 1. *Phytomedicine* 8(6), 477–480. [https://doi.org/10.1078/S0944-7113\(04\)70069-0](https://doi.org/10.1078/S0944-7113(04)70069-0)
- Guajardo-Flores D, Serna-Saldívar SO, Gutiérrez-Urbe JA (2013): Evaluation of the antioxidant and antiproliferative activities of extracted saponins and flavonols from germinated black beans (*Phaseolus vulgaris* L.). *Food Chem.* 141(2), 1497–1503. <https://doi.org/10.1016/j.foodchem.2013.04.010>
- Gupta GP, Shah Y (2021): Preparatory phase for clinical trials of COVID-19 vaccine in Nepal. *Hum. Vaccin. Immunother.* 17(2), 418–419. <https://doi.org/10.1080/21645515.2020.1809267>
- Hall DC, Jr, Ji HF (2020): A search for medications to treat COVID-19 via in silico molecular docking models of the SARS-CoV-2 spike glycoprotein and 3CL protease. *Travel Med. Infect. Dis.* 101646. <https://doi.org/10.1016/j.tmaid.2020.101646>
- Hamming I, Timens W, Bulthuis ML, Lely AT, Navis G, van Goor H (2004): Tissue distribution of ACE2 protein, the functional receptor for SARS coronavirus. A first step in understanding SARS pathogenesis. *J. Pathol.* 203(2), 631–637. <https://doi.org/10.1002/path.1570>
- Han Y, Ding Y, Xie D, Hu D, Li P, Li X, Xue W, Jin L, Song B (2015): Design, synthesis, and antiviral activity of novel rutin derivatives containing 1, 4-pentadien-3-one moiety. *Eur. J. Med. Chem.* 92, 732–737. <https://doi.org/10.1016/j.ejmech.2015.01.017>
- Herrmann EC, Jr, Kucera LS (1967): Antiviral substances in plants of the mint family (labiateae). II. Nontannin polyphenol of *Melissa officinalis*. *Proc. Soc. Exp. Biol. Med.* 124(3), 869–874. <https://doi.org/10.3181/00379727-124-31873>
- Huang S-Y, Zou X (2010): Advances and challenges in protein-ligand docking. *Int. J. Mol. Sci.* 11(8), 3016–3034. <https://doi.org/10.3390/ijms11083016>
- Huang YL, Loke SH, Hsu CC, Chiou WF (2008): (+)-Vitisin A inhibits influenza A virus-induced RANTES production in A549 alveolar epithelial cells through interference with Akt and STAT1 phosphorylation. *Planta Med.* 74(2), 156–162. <https://doi.org/10.1055/s-2007-993786>
- Huey R, Morris GM (2008): Using AutoDock 4 with AutoDocktools: a tutorial. The Scripps Research Institute, USA, 54–56.
- Huey R, Morris GM, Olson AJ, Goodsell DS (2007): A semiempirical free energy force field with charge-based desolvation. *J. Comput. Chem.* 28(6), 1145–1152. <https://doi.org/10.1002/jcc.20634>
- Hwang I-s, Lee J, Jin H-G, Woo E-R, Lee DG (2012): Amentoflavone stimulates mitochondrial dysfunction and induces apoptotic cell death in *Candida albicans*. *Mycopathologia*, 173(4), 207–218. <https://doi.org/10.1007/s11046-011-9503-x>
- Ikeda K, Nishide M, Tsujimoto K, Nagashima S, Kuwahara T, Mitani T, Koyama AH (2020): Antiviral and Virucidal Activities of Umesu Phenolics on Influenza Viruses. *Microbiol. Immunol.* 73(1), 8–13. <https://doi.org/10.7883/yoken.JJID.2018.522>
- Imran M, Rauf A, Abu-Izneid T, Nadeem M, Shariati MA, Khan IA, Imran A, Orhan IE, Rizwan M, Atif M (2019): Luteolin, a flavonoid, as an anticancer agent: A review. *Biomed. Pharmacother.* 112, 108612. <https://doi.org/10.1016/j.biopha.2019.108612>
- Izda V, Jeffries MA, Sawalha AH (2020): COVID-19: A review of therapeutic strategies and vaccine candidates. *Clin. Immunol.* 108634. <https://doi.org/10.1016/j.clim.2020.108634>
- Izda V, Jeffries MA, Sawalha AH (2021): COVID-19: A review of therapeutic strategies and vaccine candidates. *Clin. Immunol.* 222, 108634. <https://doi.org/10.1016/j.clim.2020.108634>
- Jayaraj JM, Reteti E, Kesavan C, Muthusamy K (2021): Structural insights on Vitamin D receptor and screening of new potent agonist molecules: Structure and ligand-based approach. *J. Biomol. Struct. Dyn.* 39, 4148–4159. <https://doi.org/10.1080/07391102.2020.1775122>
- Kim CH, Kim JE, Song YJ (2020): Antiviral Activities of Quercetin and Isoquercitrin Against Human Herpesviruses. *Molecules* 25(10). <https://doi.org/10.3390/molecules25102379>
- Kumar P, Erturk VS, Murillo-Arcila M (2021): A new fractional mathematical modelling of COVID-19 with the availability of vaccine. *Results Phys.* 24, 104213. <https://doi.org/10.1016/j.rinp.2021.104213>

- Lan J, Ge J, Yu J, Shan S, Zhou H, Fan S, Zhang Q, Shi X, Wang Q, Zhang L (2020): Structure of the SARS-CoV-2 spike receptor-binding domain bound to the ACE2 receptor. *Nature* 581, 215–220. <https://doi.org/10.1038/s41586-020-2180-5>
- Leib SL, Leppert D, Clements J, Täuber MG (2000): Matrix metalloproteinases contribute to brain damage in experimental pneumococcal meningitis. *Infect. Immun.* 68, 615–620. <https://doi.org/10.1128/IAI.68.2.615-620.2000>
- Leppert D, Leib S, Grygar C, Miller K, Schaad U, Holländer G (2000): Matrix metalloproteinase (MMP)-8 and MMP-9 in cerebrospinal fluid during bacterial meningitis: association with blood-brain barrier damage and neurological sequelae. *Clin. Infect. Dis.* 31(1), 80–84. <https://doi.org/10.1086/313922>
- Li LQ, Huang T (2020): COVID-19 patients' clinical characteristics, discharge rate, and fatality rate of meta-analysis. *J. Med. Virol.* 92(6), 577–583. <https://doi.org/10.1002/jmv.25757>
- Likhitwitayawuid K, Sritularak B, Benchanak K, Lipipun V, Mathew J, Schinazi RF (2005): Phenolics with antiviral activity from *Millettia erythrocalyx* and *Artocarpus lakoocha*. *Nat. Prod. Res.* 19(2), 177–182. <https://doi.org/10.1080/14786410410001704813>
- Lin Y-L, Tsai S-H, Lin-Shiau S-Y, Ho C-T, Lin J-K (1999): Theaflavin-3,3'-digallate from black tea blocks the nitric oxide synthase by down-regulating the activation of NF- $\kappa$ B in macrophages. *Eur. J. Pharmacol.* 367(2-3), 379–388. [https://doi.org/10.1016/S0014-2999\(98\)00953-4](https://doi.org/10.1016/S0014-2999(98)00953-4)
- Liu Z, Zhao J, Li W, Shen L, Huang S, Tang J, Duan J, Fang F, Huang Y, Chang H (2016): Computational screen and experimental validation of anti-influenza effects of quercetin and chlorogenic acid from traditional Chinese medicine. *Sci. Rep.* 6(1), 1–9. <https://doi.org/10.1038/srep19095>
- Ma SC, But PP, Ooi VE, He YH, Lee SH, Lee SF, Lin RC (2001): Antiviral amentoflavone from *Selaginella sinensis*. *Biol. Pharm. Bull.* 24(3), 311–312. <https://doi.org/10.1248/bpb.24.311>
- Ma SZ, Luan SH, Zhu LJ, Zhang X, Yao XS (2018): Antiviral phenolics from *Antenoron filiforme* var. *neofiliforme*. *J. Asian Nat. Prod. Res.* 20(8), 763–769. <https://doi.org/10.1080/10286020.2017.1351437>
- Malik UU, Zarina S, Pennington SR (2016): Oral squamous cell carcinoma: Key clinical questions, biomarker discovery, and the role of proteomics. *Arch. Oral Biol.* 63, 53–65. <https://doi.org/10.1016/j.archoralbio.2015.11.017>
- Meo S, Bukhari I, Akram J, Meo A, Klonoff D (2021): COVID-19 vaccines: comparison of biological, pharmacological characteristics and adverse effects of Pfizer/BioNTech and Moderna Vaccines. *Eur. Rev. Med. Pharmacol. Sci.* 25(3), 1663–1669.
- Min N, Leong PT, Lee RCH, Khuan JSE, Chu JJH (2018): A flavonoid compound library screen revealed potent antiviral activity of plant-derived flavonoids on human enterovirus A71 replication. *Antiviral Res.* 150, 60–68. <https://doi.org/10.1016/j.antiviral.2017.12.003>
- Moda TL (2007): Desenvolvimento de modelos in silico de propriedades de ADME para a triagem de novos candidatos a fármacos. São Paulo, Brazil: Universidade de São Paulo.
- Moilanen M, Pirilä E, Grenman R, Sorsa T, Salo T (2002): Expression and regulation of collagenase-2 (MMP-8) in head and neck squamous cell carcinomas. *J. Pathol.* 197(1), 72–81. <https://doi.org/10.1002/path.1078>
- Morris GM, Goodsell DS, Halliday RS, Huey R, Hart WE, Belew RK, Olson AJ (1998): Automated docking using a Lamarckian genetic algorithm and an empirical binding free energy function. *J. Comput. Chem.* 19, 1639–1662. [https://doi.org/10.1002/\(SICI\)1096-987X\(19981115\)19:14<1639::AID-JCC10>3.0.CO;2-B](https://doi.org/10.1002/(SICI)1096-987X(19981115)19:14<1639::AID-JCC10>3.0.CO;2-B)
- Muthusamy K, Prasad S, Nagamani S (2016): Role of Hydrophobic Patch in LRP6: A Promising Drug Target for Alzheimer's disease. *Indian J. Pharm. Sci.* 78(2), 240–251. <https://doi.org/10.4172/pharmaceutical-sciences.1000109>
- Naczek M, Shahidi F (2006): Phenolics in cereals, fruits and vegetables: Occurrence, extraction and analysis. *J. Pharm. Biomed. Anal.* 41(5), 1523–1542. <https://doi.org/10.1016/j.jpba.2006.04.002>
- Nagai T, Suzuki Y, Tomimori T, Yamada H (1995): Antiviral activity of plant flavonoid, 5,7,4'-trihydroxy-8-methoxyflavone, from the roots of *Scutellaria baicalensis* against influenza A (H3N2) and B viruses. *Biol. Pharm. Bull.* 18(2), 295–299. <https://doi.org/10.1248/bpb.18.295>
- Ndongo JT, Issa ME, Messi AN, Ngo Mbing J, Cuendet M, Pegenyemb DE, Bochet CG (2015): Cytotoxic flavonoids and other constituents from the stem bark of *Ochna schweinfurthiana*. *Nat. Prod. Res.* 29(17), 1684–1687. <https://doi.org/10.1080/14786419.2014.991321>
- Nishide M, Ikeda K, Mimura H, Yoshida M, Mitani T, Hajime Koyama A (2019): Antiviral and virucidal activities against herpes simplex viruses of umesu phenolics extracted from Japanese apricot. *Microbiol. Immunol.* 63(9), 359–366. <https://doi.org/10.1111/1348-0421.12729>
- Ozkan K (2020): How close are we to a Covid-19 vaccine. *J. Pure Appl. Microbiol.* 14, 1–10. <https://doi.org/10.22207/JPAM.14.SPL1.26>
- Palma M, Piñeiro Z, Barroso CG (2002): In-line pressurized-fluid extraction-solid-phase extraction for determining phenolic compounds in grapes. *J. Chromatogr A.* 968(1-2), 1–6. [https://doi.org/10.1016/S0021-9673\(02\)00823-3](https://doi.org/10.1016/S0021-9673(02)00823-3)
- Pang JY, Zhao KJ, Wang JB, Ma ZJ, Xiao XH (2014): Green tea polyphenol, epigallocatechin-3-gallate, possesses the antiviral activity necessary to fight against the hepatitis B virus replication in vitro. *J. Zhejiang Univ. Sci. B.* 15(6), 533–539. <https://doi.org/10.1631/jzus.B1300307>
- Pieper U, Webb BM, Dong GQ, Schneidman-Duhovny D, Fan H, Kim SJ, Khuri N, Spill YG, Weinkam P, Hammel M (2014): ModBase, a database of annotated comparative protein structure models and associated resources. *Nucleic Acids Res.* 42(D1), D336–D346. <https://doi.org/10.1093/nar/gkt1144>
- Ramírez-Jiménez A, Reynoso-Camacho R, Mendoza-Díaz S, Loarca-Piña G (2014): Functional and technological potential of dehydrated *Phaseolus vulgaris* L. flours. *Food Chem.* 161, 254–260. <https://doi.org/10.1016/j.foodchem.2014.04.008>

- Russo M, Moccia S, Spagnuolo C, Tedesco I, Russo GL (2020): Roles of flavonoids against coronavirus infection. *Chem. Biol. Interact.* 109211. <https://doi.org/10.1016/j.cbi.2020.109211>
- Saranraj P, Behera SS, Ray RC (2019): Traditional Foods From Tropical Root and Tuber Crops: Innovations and Challenges. *Innovations in traditional foods.* 159–191. <https://doi.org/10.1016/B978-0-12-814887-7.00007-1>
- Semple SJ, Nobbs SF, Pyke SM, Reynolds GD, Flower RL (1999): Antiviral flavonoid from *Pterocaulon sphacelatum*, an Australian Aboriginal medicine. *J. Ethnopharmacol.* 68, 283–288. [https://doi.org/10.1016/S0378-8741\(99\)00050-1](https://doi.org/10.1016/S0378-8741(99)00050-1)
- Seong RK, Kim JA, Shin OS (2018): Wogonin, a flavonoid isolated from *Scutellaria baicalensis*, has anti-viral activities against influenza infection via modulation of AMPK pathways. *Acta Virol.* 62, 78–85. <https://doi.org/10.4149/av.2018.109>
- Serkedzhieva I, Manolova N (1988): The antiviral action of a polyphenol complex isolated from the medicinal plant *Geranium sanguineum* L. VI. Reproduction of the influenza virus pretreated with the polyphenol complex. *Acta Microbiol. Bulg.* 22, 16–21.
- Serkedzhieva I, Manolova N, Gegova G, Maksimova-Todorova V, Ivancheva S (1986a): Antiviral action of a polyphenol complex isolated from the medicinal plant *Geranium sanguineum* L. II. Its inactivating action on the influenza virus. *Acta Microbiol. Bulg.* 18, 78–82.
- Serkedzhieva I, Manolova N, Maksimova-Todorova V, Gegova G (1986b): Combined action of antiviral substances of natural and synthetic origin. I. The anti-influenza action of a combination of the polyphenol complex isolated from *Geranium sanguineum* L. and remantadine in vitro and in ovo. *Acta Microbiol. Bulg.* 19, 18–22.
- Shen L, Yang W (2018): Molecular dynamics simulations with quantum mechanics/molecular mechanics and adaptive neural networks. *J. Chem. Theory Comput.* 14, 1442–1455. <https://doi.org/10.1021/acs.jctc.7b01195>
- Shi F, Yu Q, Huang W, Tan C (2020): 2019 Novel Coronavirus (COVID-19) Pneumonia with Hemoptysis as the Initial Symptom: CT and Clinical Features. *J. Korean Soc. Radiol.* 21, 537–540. <https://doi.org/10.3348/kjr.2020.0181>
- Silva VBd (2008): Estudos de modelagem molecular e relação estrutura atividade da oncoproteína hnRNP K e ligantes. São Paulo, Brazil: Universidade de São Paulo.
- Sokmen M, Angelova M, Krumova E, Pashova S, Ivancheva S, Sokmen A, Serkedjjeva J (2005): In vitro antioxidant activity of polyphenol extracts with antiviral properties from *Geranium sanguineum* L. *Life Sci.* 76, 2981–2993. <https://doi.org/10.1016/j.lfs.2004.11.020>
- Sung MJ, Davaatseren M, Kim W, Park SK, Kim SH, Hur HJ, Kim MS, Kim YS, Kwon DY (2009): Vitisin A suppresses LPS-induced NO production by inhibiting ERK, p38, and NF-kappaB activation in RAW 264.7 cells. *Int. Immunopharmacol.* 9, 319–323. <https://doi.org/10.1016/j.intimp.2008.12.005>
- Taherkhani A, Moradkhani S, Orangi A, Jalalvand A, Khamverdi Z (2020): Molecular docking study of flavonoid compounds for possible matrix metalloproteinase-13 inhibition. *J. Basic Clin. Physiol. Pharmacol.* 1 (ahead-of-print). <https://doi.org/10.1515/jbcpp-2020-0036>
- Taherkhani A, Orangi A, Moradkhani S, Khamverdi Z (2021): Molecular Docking Analysis of Flavonoid Compounds with Matrix Metalloproteinase-8 for the Identification of Potential Effective Inhibitors. *Lett. Drug Des. Discov.* 18; 16–45. <https://doi.org/10.2174/1570180817999200831094703>
- Ulomskiy EN, Ivanova AV, Gorbunov EB, Esaulkova IL, Slita, AV, Sinegubova, EO, Voinkov, EK, Drokin, RA, Butorin II, Gazizullina ER, Gerasimova EL, Zarubaev VV, Rusinov VL (2020): Synthesis and biological evaluation of 6-nitro-1,2,4-triazoloazines containing polyphenol fragments possessing antioxidant and antiviral activity. *Bioorg. Med. Chem. Lett.* 30(13), 127216. <https://doi.org/10.1016/j.bmcl.2020.127216>
- Van Lint P, Libert C (2006): Matrix metalloproteinase-8: cleavage can be decisive. *Cytokine Growth Factor Rev.* 17(4), 217–223. <https://doi.org/10.1016/j.cytogfr.2006.04.001>
- Wang W, Guo J, Zhang J, Peng J, Liu T, Xin Z (2015): Isolation, identification and antioxidant activity of bound phenolic compounds present in rice bran. *Food Chem.* 171, 40–49. <https://doi.org/10.1016/j.foodchem.2014.08.095>
- Wong KY, Abd El-Aziz TM, Stockand JD (2020): Recent progress and challenges in drug development against COVID-19 coronavirus (SARS-CoV-2) – an update on the status. *Infect. Genet. Evol.* 83, 104327. <https://doi.org/10.1016/j.meegid.2020.104327>
- Wujtewicz M, Dylczyk-Sommer A, Aszkiełowicz A, Zdanowski S, Piwowarczyk S, Owczuk, R (2020): COVID-19 – what should anaesthesiologists and intensivists know about it? *Anaesthesiol Intensive Ther.* 52(1), 34–41. <https://doi.org/10.5114/ait.2020.93756>
- Xiong H-R, Shen Y-Y, Lu L, Hou W, Luo F, Xiao H, Yang Z-Q (2012): The inhibitory effect of *Rheum palmatum* against coxsackievirus B3 in vitro and in vivo. *Am. J. Chinese Med.* 40(04), 801–812. <https://doi.org/10.1142/S0192415X12500607>
- Xu X, Chen P, Wang J, Feng J, Zhou H, Li X, Zhong W, Hao P (2020): Evolution of the novel coronavirus from the ongoing Wuhan outbreak and modeling of its spike protein for risk of human transmission. *Sci. China Life Sci.* 63(3), 457–460. <https://doi.org/10.1007/s11427-020-1637-5>
- Yamashita F, Hashida M (2004): In silico approaches for predicting ADME properties of drugs. *Drug Metab. Pharmacokinet.* 19(5), 327–338. <https://doi.org/10.2133/dmpk.19.327>
- Yin D, Li J, Lei X, Liu Y, Yang Z, Chen K (2014): Antiviral Activity of Total Flavonoid Extracts from *Selaginella moellendorffii* Hieron against Coxsackie Virus B3 In Vitro and In Vivo. *Evid. Based Complement. Alternat. Med.* 2014, 950817. <https://doi.org/10.1155/2014/950817>
- Yu S, Yan H, Zhang L, Shan M, Chen P, Ding A, Li SFY (2017): A review on the phytochemistry, pharmacology, and pharmacokinetics of amentoflavone, a naturally-occurring biflavonoid. *Molecules* 22(2), 299. <https://doi.org/10.3390/molecules22020299>

## COVID-19: docking-based virtual screening and molecular dynamics study to identify potential SARS-CoV-2 spike protein inhibitors from plant-based phenolic compounds

Shirin Moradkhani<sup>1</sup>, Abbas Farmani<sup>2</sup>, Massoud Saidijam<sup>3</sup>, Amir Taherkhani<sup>4\*</sup>

<sup>1</sup>Department of Pharmacognosy, School of Pharmacy, Medicinal Plants and Natural Product Research Center, Hamadan University of Medical Sciences, Hamadan, Iran; <sup>2</sup>Dental Research Center, Hamadan University of Medical Sciences, Hamadan, Iran; <sup>3</sup>Department of Molecular Medicine and Genetics, Research Center for Molecular Medicine, Hamadan University of Medical Sciences, Hamadan, Iran; <sup>4</sup>Research Center for Molecular Medicine, Hamadan University of Medical Sciences, Hamadan, Iran

Received January 26, 2021; revised April 29, 2021; accepted July 20, 2021

**Table S1. Estimated free energy of binding and inhibition constant for 97 flavonoids after docking with spike protein receptor binding domain**

PubChem ID	Ligand name	Estimated free energy of binding (kcal/mol)	Inhibition constant
16131430	Vitisin A	-11.99	1.62 nM
135403795	Theaflavin 3,3'-digallate	-11.26	5.57 nM
135430431	Vitisin A	-10.95	9.33 nM
442664	Vicenin-2	-10.73	13.53 nM
10621	Hesperidin	-10.45	21.90 nM
119258	Astilbin	-10.38	24.52 nM
5280805	Rutin	-10.1	39.46 nM
135403798	Theaflavin	-10.09	40.27 nM
5281600	Amentoflavone	-10.05	42.89 nM
71623698	Prodelphinidin C2	-9.64	86.33 nM
442428	Naringin	-9.37	136.46 nM
441765	Malvin	-9.37	135.50 nM
29231	Keracyanin	-9.32	148.50 nM
5089687	Prodelphinidin B3	-9.16	193.07 nM
44257662	Vicenin 1	-9.15	195.21 nM
169853	Procyanidin C1	-9.01	247.06 nM
185958	Vicenin 3	-8.87	314.42 nM
5318767	Nicotiflorin	-8.72	405.09 nM

\*Corresponding author. E-mail: amir.007.taherkhani@gmail.com, amir\_007\_taherkhani@yahoo.com, a.taherkhani@umsha.ac.ir; phone: +98-9183145963.

Table S1. Continued 1

PubChem ID	Ligand name	Estimated free energy of binding (kcal/mol)	Inhibition constant
442439	Neohesperidin	-8.68	430.57 nM
5280804	Isoquercitrin	-8.52	567.08 nM
5388496	Punicalin	-8.51	575.45 nM
11250133	Procyanidin B1	-8.45	636.23 nM
5281675	Orientin	-8.35	755.91 nM
5281377	Genistin	-8.12	1.13 uM
442543	Theasinensin A	-8.09	1.18 uM
13644663	Vicenin 1	-8.03	1.30 uM
5280459	Quercitrin	-7.89	1.64 uM
5280441	Vitexin	-7.86	1.72 uM
196402	$\alpha$ -Viniferin	-7.82	1.86 uM
5280704	Apigenin-7-glucoside	-7.76	2.04 uM
5486172	Puerarin	-7.66	2.43 uM
134715108	Procyanidin A1	-7.56	2.86 uM
107905	Epicatechin gallate	-7.52	3.06 uM
5353915	Quercetin-3-rhamnoside	-7.48	3.29 uM
107971	Daidzin	-7.18	5.48 uM
443651	Petunidin 3-glucoside	-7.12	6.04 uM
65064	Epigallocatechin gallate	-7	7.42 uM
5281728	Epsilon-Viniferin	-6.96	7.90 uM
443654	Peonidin-3-glucoside	-6.88	9.04 uM
145937	Eckol	-6.83	9.91 uM
443648	Pelargonidin 3-glucoside	-6.83	9.87 uM
132944	Selligueain A	-6.71	12.03 uM
6438825	Brousochalcone A	-6.65	13.43 uM
16129869	Punicalagin	-6.64	13.54 uM
629440	Hemileiocarpin	-6.51	16.91 uM
5281605	Baicalein	-6.44	19.15 uM
14033983	Karanjachromene	-6.31	23.78 uM
5281814	Wighteone	-6.28	25.01 uM
5490139	Alpinumisoflavone	-6.17	29.85 uM
439533	Taxifolin	-6.08	35.00 uM
162807	Glyceollin I	-5.97	41.88 uM
5320945	Rhamnazin	-5.93	45.01 uM
100633	Karanjin	-5.9	47.31 uM
5281654	Isorhamnetin	-5.89	47.94 uM
9817274	Sappanone A	-5.89	48.30 uM
480774	Glabrene	-5.84	52.08 uM
5281855	Ellagic acid	-5.83	53.53 uM
159287	Malvidin	-5.72	64.63 uM
439246	Naringenin	-5.67	70.37 uM
124052	Glabridin	-5.66	70.73 uM

Table S1. Continued 2

PubChem ID	Ligand name	Estimated free energy of binding (kcal/mol)	Inhibition constant
5280343	Quercetin	-5.62	76.05 uM
5281255	Isobavachalcone	-5.59	79.27 uM
969516	Curcumin	-5.57	82.44 uM
5281672	Myricetin	-5.55	85.24 uM
16212782	Fisetinidin chloride	-5.55	84.80 uM
114829	Liquiritigenin	-5.53	88.13 uM
164762	Leuco-fisetinidin	-5.52	90.65 uM
122850	Aromadendrin	-5.51	91.20 uM
5280445	Luteolin	-5.5	93.28 uM
5281607	Chrysin	-5.43	104.57 uM
9064	Catechin	-5.39	111.68 uM
5280544	Herbacetin	-5.37	115.40 uM
5318998	licochalcone a	-5.36	118.70 uM
443639	Epiafzelechin	-5.35	119.09 uM
5281616	Galangin	-5.31	128.43 uM
5280863	Kaempferol	-5.3	130.91 uM
638278	Isoliquiritigenin	-5.3	50.32 uM
65084	Gallocatechol	-5.3	131.38 uM
639665	Xanthohumol	-5.27	138.19 uM
1203	Epicatechin	-5.25	141.93 uM
5280443	Apigenin	-5.24	145.05 uM
5281707	Coumestrol	-5.21	151.18 uM
5281708	Daidzein	-5.15	168.99 uM
68245	Delphinidin chloride	-5.07	190.63 uM
14309735	Xanthogalenol	-5.01	213.41 uM
5280961	Genistein	-5.01	213.31 uM
129648	Glycinol	-4.99	220.95 uM
68077	Tangeretin	-4.96	229.69 uM
10207	Aloe emodin	-4.91	250.84 uM
5280378	Formononetin	-4.84	283.55 uM
3220	Emodin	-4.83	288.31 uM
1548910	Cis-Resveratrol	-4.76	324.12 uM
445154	Resveratrol	-4.3	709.97 uM
370	Gallic acid	-3.91	1.35 mM
359	Phloroglucinol	-3.29	3.87 mM
64982	Baicalin	-1.72	55.17 mM
5317050	Geranin A	1	NA

**Table S2. Two dimensional structures and the main sources of top nine phenolic inhibitors of SARS-CoV-2 spike protein RBD**

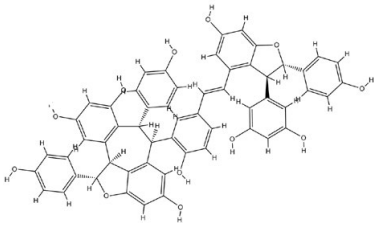
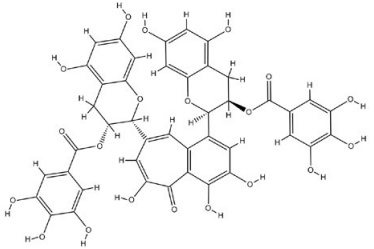
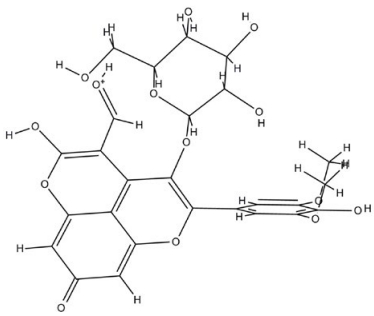
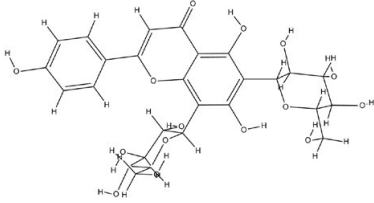
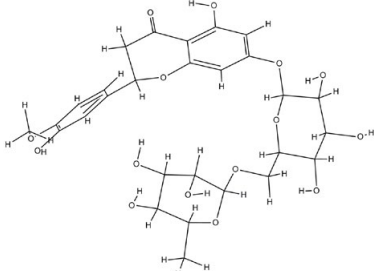
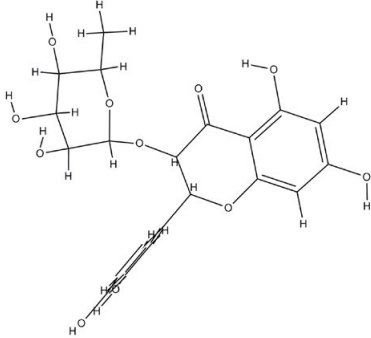
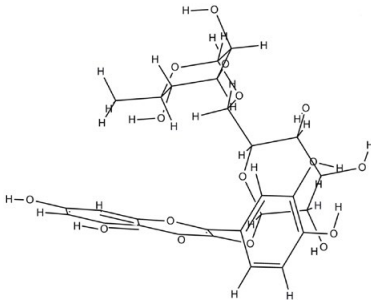
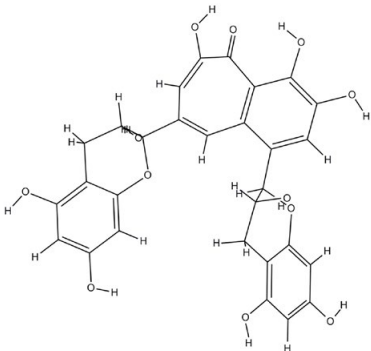
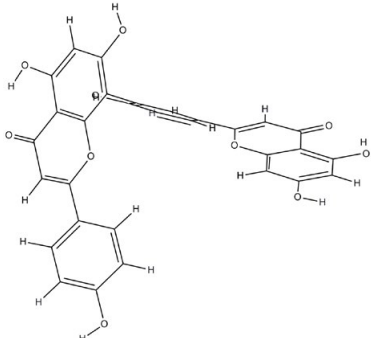
PubChem ID	Ligand name	Two dimensional Structure	Source	Reference
16131430	Vitisin A		The CDX and the JPG file has been sent separately: It could not be pasted here	Vitis vinifera roots (1)
135403795	Theaflavin 3,3'-digallate		The CDX and the JPG file has been sent separately: It could not be pasted here	Black tea (2)
135430431	Vitisin A (pyranoanthocyanin)		The CDX and the JPG file has been sent separately: It could not be pasted here	Vitis vinifera roots (1)
442664	Vicenin 2		The CDX and the JPG file has been sent separately: It could not be pasted here	Aerial parts of urtica circularis (3)
10621	Hesperidin		The CDX and the JPG file has been sent separately: It could not be pasted here	Citrus fruits (4)

Table S2. Continued

PubChem ID	Ligand name	Two dimensional Structure	Source	Reference
119258	Astilbin	 The CDX and the JPG file has been sent separately: It could not be pasted here	Rhizome of smilax china L	(5)
5280805	Rutin	 The CDX and the JPG file has been sent separately: It could not be pasted here	Vegetables and and beverages	(6)
135403798	Theaflavin	 The CDX and the JPG file has been sent separately: It could not be pasted here	Black tea	(7)
5281600	Amentoflavone	 The CDX and the JPG file has been sent separately: It could not be pasted here	Selaginella tamariscina, cupressus funebris, ginkgo biloba, and hypericum perforatum	(8)

SARS-CoV-2, Severe acute respiratory syndrome coronavirus 2; RBD, receptor binding domain.

### References

- Mi Jeong S, Davaatseren M, Kim W, Sung Kwang P, Kim SH, Haeng Jeon H, et al. Vitisin A suppresses LPS-induced NO production by inhibiting ERK, p38, and NF-kappaB activation in RAW 264.7 cells. *International immunopharmacology*. 2009; 9(3): 319-233.
- Liu S, Lu H, Zhao Q, He Y, Niu J, Debnath AK, et al. Theaflavin derivatives in black tea and catechin derivatives in green tea inhibit HIV-1 entry by targeting gp41. *Biochimica et biophysica acta*. 2005; 1723(1-3): 270-281.
- Marrassini C, Davicino R, Acevedo C, Anesini C, Gorzalczany S, Ferraro G. Vicenin-2, a potential anti-inflammatory constituent of *Urtica circularis*. *Journal of natural products*. 2011; 74(6): 1503-1507.
- da Silva LM, Pezzini BC, Somensi LB, Bolda Mariano LN, Mariott M, Boeing T, et al. Hesperidin, a citrus flavanone glycoside, accelerates the gastric healing process of acetic acid-induced ulcer in rats. *Chemico-biological interactions*. 2019; 308: 45-50.
- Chen L, Lan Z, Zhou Y, Li F, Zhang X, Zhang C, et al. Astilbin attenuates hyperuricemia and ameliorates nephropathy in fructose-induced hyperuricemic rats. *Planta medica*. 2011; 77(16): 1769-1773.
- Yang H, Wang C, Zhang L, Lv J, Ni H. Rutin alleviates hypoxia/reoxygenation-induced injury in myocardial cells by up-regulating SIRT1 expression. *Chemico-biological interactions*. 2019; 297: 44-49.
- Wang W, Sun Y, Liu J, Wang J, Li Y, Li H, et al. Protective effect of theaflavins on cadmium-induced testicular toxicity in male rats. *Food and chemical toxicology*. 2012; 50(9): 3243-3250.
- Lv X, Zhang J-B, Wang X-X, Hu W-Z, Shi Y-S, Liu S-W, et al. Amentoflavone is a potent broad-spectrum inhibitor of human UDP-glucuronosyltransferases. *Chemico-biological interactions*. 2018; 284: 48-55.